Murine cathepsin D deficiency is associated with dysmyelination/myelin disruption and accumulation of cholesteryl esters in the brain

Journal of Neurochemistry

JOURNAL OF NEUROCHEMISTRY | 2010 | 112 | 193–203 doi: 10.1111/j.1471-4159.2009.06440.x

Murine cathepsin D deficiency is associated with dysmyelination/myelin disruption and accumulation of cholesteryl esters in the brain

Aino-Liisa Mutka,*[,1] Aleksi Haapanen,†[,1] Reijo Käkelä,† Maria Lindfors,† Ann K. Wright,‡ Teija Inkinen,† Martin Hermansson,† Anne Rokka,§ Garry Corthals,§ Matti Jauhiainen,¶ Thomas H. Gillingwater,‡ Elina Ikonen* and Jaana Tyynelä†

*Institute of Biomedicine/Anatomy, Biomedicum, University of Helsinki, Helsinki, Finland

†Institute of Biomedicine/Biochemistry, Biomedicum, University of Helsinki, Helsinki, Finland

‡Centre for Integrative Physiology, University of Edinburgh, Edinburgh, UK

§Turku Centre for Biotechnology, University of Turku and Åbo Akademi University, Turku, Finland

¶National Institute for Health and Welfare and FIMM, Institute for Molecular Medicine Finland, Biomedicum, Helsinki, Finland

Abstract

Cathepsin D (CTSD) deficiencies are fatal neurological diseases that in human infants and in sheep are characterized by extreme loss of neurons and myelin. To date, similar morphological evidence for myelin disruption in CTSD knockout mice has not been reported. Here, we show that CTSD deficiency leads to pronounced myelin changes in the murine brain: myelin-related proteolipid protein and myelin basic protein were both markedly reduced at postnatal day 24, and the amount of lipids characteristically high in myelin (e.g. plasmalogen-derived alkenyl chains and glycosphingolipid-derived 20- and 24-carbon acyl chains) were significantly lowered compared with controls. These changes were accompanied by ultrastructural alterations of myelin, including significant thinning of myelin sheaths. Furthermore, in CTSD knockout brains there was a pronounced accumulation of cholesteryl esters and abnormal levels of proteins related to cholesterol transport, with an increased content of apolipoprotein E and a reduced content of ATP-binding cassette transporter A1. These results provide evidence for dysmyelination and altered trafficking of cholesterol in brains of CTSD knockout mice, and warrant further studies on the role of lipid metabolism in the pathogenesis of CTSD deficiencies.

Keywords: cathepsin D, lipidomics, mouse model, myelin, proteomics, ultrastructure.

J. Neurochem. (2010) **112**, 193–203.

Mutations in the cathepsin D (*CTSD*) gene underlie the congenital neuronal ceroid-lipofuscinosis, a fatal neurodegenerative disease occurring in humans and in sheep (Tyynela *et al.* 2000; Siintola *et al.* 2006; Fritchie *et al.* 2008). The brains of the affected infants and lambs are extremely atrophic already at birth, showing extensive loss of neurons and myelin, pronounced gliosis and accumulation of lipofuscin within the remaining cells (Norman and Wood 1941; Tyynela *et al.* 2000; Siintola *et al.* 2006; Fritchie *et al.* 2008). These are accompanied by signs of developmental delay (Norman and Wood 1941; Garborg *et al.* 1987; Tyynela *et al.* 2000; Fritchie *et al.* 2008).

Ctsd knockout (−/−) mice, generated by gene targeting, also develop a neurological disease, although the course of the disease is milder than in man or sheep. Nevertheless, the mice have epilepsy and die prematurely at the age of 25 ± 1 days (Saftig *et al.* 1995; Koike *et al.* 2000). At the terminal age of 24 days, *Ctsd*−/− mice show neuropathological changes resembling those in the human patients, including accumulation of storage material in neurons and neurodegeneration,

Received July 13, 2009; revised manuscript received October 10, 2009; accepted October 13, 2009.

Address correspondence and reprint requests to Jaana Tyynelä, Institute of Biomedicine/Biochemistry, POB 63, FIN-00014, University of Helsinki, Helsinki, Finland. E-mail: jaana.tyynela@helsinki.fi

[1]Both these authors contributed equally to this study.

Abbreviations used: ABCA1, ATP-binding casette transporter A1; ApoE, apolipoprotein E; CNP, 2′,3′-cyclic nucleotide 3′-phosphodiesterase; CTSD, cathepsin D; EM, electron microscopy; IPG, immobilized pH gradient; iTRAQ, isobaric tags for absolute and relative quantitation; LFB, Luxol fast blue; MBP, myelin basic protein; MS, mass spectrometry; P24, postnatal day 24; PC, principal component; PE, phosphatidylethanolamine; PLP, proteolipid protein; SAP, sphingolipid activator protein.

particularly within the thalamus, hippocampus, and the deep laminae of the cerebral cortex (Koike *et al.* 2000; Partanen *et al.* 2008). Recent *in vivo* magnetic resonance imaging studies indicated that corpus callosum, the largest individual white matter structure of the mouse brain, was profoundly atrophic in the *Ctsd*−/− mice (Haapanen *et al.* 2007). Furthermore, disruption of the myelin sheaths within the thalamus of these mice was revealed by electron microscopy (EM) (Partanen *et al.* 2008). Together these data suggest that pathological alterations occur not only in the brains of man and sheep with CTSD deficiency, but also within the white matter of *Ctsd*−/− mice. Interestingly, *Ctsd*−/− mice begin to show clinical sings (including epilepsy) around 2 weeks of age, and neuropathological alterations around postnatal day 19 (P19) (Haapanen *et al.* 2007). Thus, the clinico-pathological deterioration of these mice coincides with the active period of synaptogenesis and myelination that take place after the first postnatal week in the mouse brain (Saher *et al.* 2005).

The myelination process markedly affects the brain lipid profile. The levels of alkenyl-acyl species of phosphatidylethanolamines, also called ethanolamine plasmalogens, and glycosphingolipids with 20- and 24-carbon acyl chains increase with the degree of myelination (Rao 1977; Jurevics and Morell 1995). Cholesterol is an important structural component of myelin (Saher *et al.* 2005) and myelination is associated with enhanced synthesis of cholesterol in the CNS (Jurevics and Morell 1995). After myelination has been completed, cholesterol synthesis settles to a lower, steady state level. Besides cholesterol, brain lipids consist of two other major categories: glycerophospholipids (e.g. phosphatidylcholine, phosphatidylethanolamine, phosphatidylserine, and phosphatidylinositol) and sphingolipids (sphingomyelin and glycosphingolipids: cerebrosides, sulfatides, globosides, and gangliosides). Interestingly, Jabs *et al.* (2008) reported increased levels of certain gangliosides and bis(monoacylglycero) phosphate in the brain of *Ctsd*−/− mice, connected in conjunction with accumulation of lysosomal storage material.

To clarify the molecular events related to the myelin pathology occurring in *Ctsd*−/− mice, we have here investigated the morphology of myelin, lipid profile and lipid-related proteins in the brains of these mice using ultrastructural, immunological, lipidomic and proteomic methods. Our data reveal major alterations not only in the myelin content but also in the overall lipid metabolism in the brains of *Ctsd*−/− mice compared with controls, suggesting that CTSD is needed for the maintenance and regulation of normal lipid homeostasis, particularly cholesterol homeostasis, in the brain.

Materials and methods

Animals

Ctsd−/− mice (Saftig *et al.* 1995) were maintained on a mixed C57BL6J strain background in the animal facility of the Helsinki University, Biomedicum, where food and water were available *ad libitum* and light/dark cycle was 12/12 h. The study protocol was approved by the Ethical Committee of the University of Helsinki.

Antibodies

The following antibodies were used for semi-quantitative western blotting: Rabbit polyclonal antibodies against murine apolipoprotein A–I (ApoA–I) (van Haperen *et al.* 2000), murine ApoE (raised against purified mouse plasma ApoE protein) and ATP-binding casette transporter A1 (ABCA1) (Novus Biologicals, Littleton, CO, USA) were used for western blotting where indicated. For immunohistochemical staining of paraffin sections, mouse monoclonal antibodies against myelin proteolipid protein (PLP; Abcam, Cambridge, UK) and rabbit polyclonal antibodies against myelin basic protein (MBP; Dako, Cambridge, UK) were used.

Histological processing and staining of brain samples

For paraffin-embedded samples, brains from 23 ± 1-day-old *Ctsd*−/− and *Ctsd* wild-type (+/+) mice (n = 5 for each genotype) were fixed in 4% neutral-buffered formaldehyde and subsequently processed, embedded in paraffin and cut into 4 or 8 μm thick sections. Four micrometer thick sections of the paraffin-embedded *Ctsd*−/− and control mouse brain were immunohistochemically stained with the relevant antibodies. Sections were dewaxed in xylene, antigen retrieval for MBP staining was performed by microwaving the sections in citric acid buffer, and endogenous peroxidase activity was blocked by incubating the sections in methanol containing 1.6% H_2O_2 at 20°C for 30 min. Sections were blocked and stained for each antigen using the appropriate Vectastain Elite kit (Vector Laboratories, Peterborough, UK), and immunoreactivity was visualized using 3-amino-9-ethylcarbazole and H_2O_2. Before mounting, the sections were counterstained with hematoxylin. Luxol fast blue (LFB) staining was performed for 8 μm thick sections.

Electron microscopy

Ctsd−/− and wild-type mice at P23/24 were anesthetized using subcutaneous injection of ketamine (75-100 mg/kg; Orion Pharma, Espoo, Finland) and killed by perfusion fixation with 0.1 M phosphate buffer, pH 7.4, containing 4% *p*-formaldehyde/2.5% glutaraldehyde. Brains were processed for EM as described previously (Gillingwater *et al.* 2006). Morphometric measurements (including axon diameter and myelin sheath thickness) were made from digital micrographs using IMAGE J software (version 1.35c, developed by Wayne Rasband, NIH, USA, http://rsb.info.nih.gov/ij/) with data collected and analyzed using Microsoft (Redmont, WA, USA) Excel software and GRAPHPAD PRISM software (GraphPad Software Inc., San Diego, CA, USA). For each fiber, the g ratio was calculated as d/D, where d was the axon diameter and D was twice the myelin sheath thickness (Fraher and O'Sullivan 2000).

Western blot analysis

The cerebral cortices of control and *Ctsd*−/− and *Ctsd*+/+ mice were homogenized in 50 mM Tris, pH 7.0, containing 0.6% sodium dodecyl sulfate, 1.5 M thiourea, 5 M urea, 3% 3-[(3-Cholamidopropyl)Dimethyl-Ammonio]-1-Propanesulfonate, and 0.7% dithiotreitol. The homogenates were centrifuged at 1700 g, for 10 min at 4°C, the supernatants collected, and protein concentrations determined using the bicinchoninic acid protein kit (Interchim,

Montluçon, France). Twenty microgram of protein from each homogenate was subjected to 6–12% sodium dodecyl sulfate–polyacrylamide gel electrophoresis, as appropriate for the expected molecular weights, in the presence of β-mercaptoethanol. The gels were blotted onto Hybond C nitrocellulose filters, blocked with 5% defatted milk in Tris-buffered saline–0.1% Tween 20 and incubated with the primary antibodies overnight at 4°C. Immunoreactive bands were visualized by enhanced chemiluminescence after incubation with goat anti-rabbit IgG coupled to horseradish peroxidase (Bio-Rad, Hercules, CA USA). The intensities of the bands were quantified using TINA 2.1 software (Raytest, Pittsburgh, PA, USA).

Proteomics

The cerebra of two to three mice of both genotypes (*Ctsd*−/− and *Ctsd*+/+ mice) were collected at P24, combined and homogenized by 10 strokes with a Teflon-glass homogenizer in 320 mM sucrose/1 mM $MgCl_2$/0.5 mM $CaCl_2$/4 mM HEPES, pH 7.3 (using 4 mL of buffer per 1 g of tissue). Synaptosomes were isolated from these homogenates as described previously (Suopanki *et al.* 2002). The protein content of the crude synaptosomal fractions was determined by the bicinchoninic acid method.

Differences in the apparent relative concentration of proteins between *Ctsd*−/− and *Ctsd*+/+ mouse synaptosomes were measured by mass spectrometry (MS) based isobaric tags for absolute and relative quantitation (iTRAQ) labeling method (Ross *et al.* 2004). For this purpose, equal amounts of synaptosomal proteins (100 μg) were precipitated with six volumes of cold acetone at −20°C for 2 h and the pellets were dissolved in triethylammonium bicarbonate buffer provided with the 4-plex iTRAQ kit (Applied Biosystems, Foster City, CA, USA). Reduction, alkylation, trypsin digestion, and iTRAQ labeling were performed according to the manufacturer's protocol. After labeling, the peptide samples from *Ctsd*−/− and +/+ mice were pooled, desalted using C18 Empore disks (3M; St Paul, MN, USA), and dried. To fractionate the peptides based on their pI, the peptide samples were dissolved in immobilized pH gradient (IPG) strip rehydration solution [4 M urea, 2% (v/v) IPG buffer, pH 3–10] and loaded on a 13 cm IPG strip (GE Healthcare, Amersham Biosciences, Uppsala, Sweden) with a pH gradient 3–10. Electrofocusing of peptides was performed with IPGphor (GE Healthcare, Amersham Biosciences) until 20 kVh. After focusing, the strip was cut into 12 fractions, peptides were extracted according to Cargile *et al.* (2004) and desalted again to remove urea. Liquid chromatography–MS/MS analyses were performed on a nanoflow LC system (Famos, Switchos and Ultimate, LC Packings/MDS Sciex, Sunnyvale, CA, USA) coupled to a QSTAR Pulsar *i* MS (Applied Biosystems/MDS Sciex, Toronto, ON, Canada). Peptides were first loaded on a pre-column (0.3 × 5 mm PepMap C18; LC Packings, Sunnyvale, CA, USA) and then separated on a 15 cm C18 column (75 μm × 15 cm, Magic 5 μm 100 Å C_{18}; Michrom BioResources Inc., Auburn, CA, USA). A linear 120 min gradient (from 2% to 34% acetonitrile) was used to elute peptides. Data acquisition parameters suggested by Applied Biosystems were used. Protein PILOT software (version 1.0; Applied Biosystems) was used for protein identification and quantification. This software compares the relative intensity of proteins present in *Ctsd*−/− and control samples based on the intensity of reporter ions released from each labeled peptide, and automatically calculates the quantity ratios and *p*-values for each protein. Database searches were carried out against Swiss Prot–Trembl, taxonomy mouse.

Analysis of neutral lipids

Snap-frozen dissected frontal lobes from P24 *Ctsd*−/− *and Ctsd*+/+ mice were allowed to thaw on ice. They were then homogenized into 2% NaCl and aliquots were taken for protein determination. The protein concentrations were determined according to (Lowry *et al.* 1951). Lipids were extracted according to Bligh and Dyer (1959), and the samples were adjusted for protein concentration and applied on HPTLC Silica Gel 60 F524 plates (Merck, Darmstadt, Germany) by using an automatic TLC sampler 4 (Camag, Berlin, Germany). Lipids on TLC plates were resolved by using hexane/diethyl ether/acetic acid (80 : 20 : 1) as solvent. Lipids were visualized by staining with 3% copper sulfate and 8% phosphoric acid, followed by heating at 180°C for 5 min. The intensity of the bands was quantified using TINA 2.1 software (Raytest).

Analysis of polar lipids and fatty acyl and alkenyl chain composition

Snap-frozen samples of cerebral cortices (rostral and caudal parts) of the *Ctsd*−/− and +/+ mice were extracted according to Folch *et al.* (Folch *et al.* 1957). The total phospholipid and cholesterol content in the brain lipid extracts was studied by spectrophotometric methods (Bartlett and Lewis 1970, Gamble *et al.* 1978). The acyl and alkenyl chain composition of brain total lipids was determined by GLC (Kakela *et al.* 2005). Aliquots of the total lipid extracts were spiked with a cocktail of 18 phospholipid and sphingolipid standards, and analyzed by liquid chromatography–MS (Kakela *et al.* 2003; Hermansson *et al.* 2005). The lipid molecular species were identified and quantified as detailed previously (Hermansson *et al.* 2005; Haimi *et al.* 2006). The acyl-acyl and alkenyl-acyl pairs in each phospholipid species were studied by acyl chain specific daughter scans and analysis of product ions produced upon fragmentation (Kainu *et al.* 2008).

Statistics

The differences in the relative amounts of the phospholipid molecular species, amounts of neutral lipids and signal intensities in the semi-quantitative western blots in *Ctsd*−/− and +/+ mouse brains were studied by Student's *t*-test. Multivariate principal component (PC) analysis was applied to compare the fatty acyl and alkenyl chain composition of the brain samples (Kvalheim and Karstang 1987). Prior to the analysis, the molar percentages of the acyl and alkenyl chains were logarithmically transformed to prevent the abundant components with large variance from dominating the analysis. The samples positioned in multidimensional space were plotted in two new coordinates (PC1 and PC2) calculated to describe the largest and second largest variance of the data among the samples. The computations were performed by using SIRIUS program package (Pattern Recognition Systems, Bergen, Norway).

Results

Histochemistry and immunohistochemistry

Cathepsin D deficiencies in human infants and newborn lambs are characterized by extreme loss of myelin. In *Ctsd*−/− mouse brains, however, myelin loss is not readily evident without specific stainings against myelin lipids or

proteins. To examine the myelinated structures in *Ctsd*−/− and *Ctsd*+/+ (control) mouse brains, we stained paraffin-embedded brain slices with the classical LFB method and with antibodies against two major myelin proteins, the MBP and PLP (Fig. 1). There were no gross differences in the LFB and MBP staining between *Ctsd*−/− mice and controls at the terminal stage of the disease, P24 (not shown). In contrast, PLP staining was markedly reduced in the affected mice, this being particularly apparent in the striatum (not shown), corpus callosum, and hippocampus (Fig. 1a). In the thalamus of the *Ctsd*−/− mice, the PLP staining appeared in abnormal clusters instead of the finely punctate fibers typically seen in the control mice (Fig. 1a). In a compact white matter structure, the anterior commisura, where the stainings are easy to compare, PLP and LFB staining intensity was clearly reduced in *Ctsd*−/− mice compared with controls, while MBP staining appeared nearly normal in the affected mice (Fig. 1b).

Electron microscopy

As PLP and LFB stainings revealed myelin-specific changes in the *Ctsd*−/− mice, we used EM to qualitatively and quantitatively examine axon and myelin morphology in the corpus callosum of these mice. Qualitatively, micrographs from the corpus callosum of control mice showed intact axons and myelin sheaths (Fig. 2a). By contrast, micrographs from *Ctsd*−/− mice showed reduced numbers of axon profiles, widespread axonal degeneration (evidenced by disrupted axon membranes and organelles) and modifications in myelin integrity and thickness (Fig. 2b). In particular,

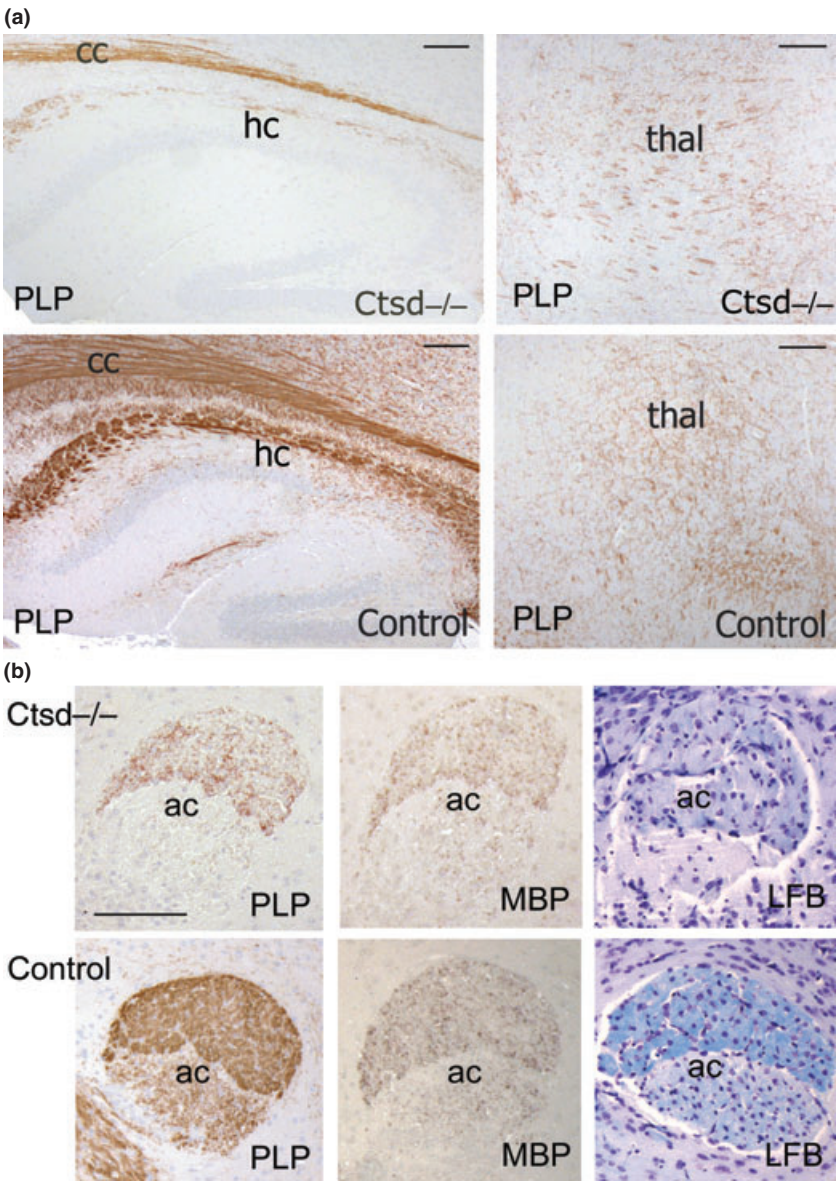

Fig. 1 Histochemical and immunohistochemical staining of paraffin-embedded mouse brains. (a) Immunohistological staining of paraffin-embedded mouse brains with antibodies against proteolipid protein (PLP). In control mouse brains, the PLP staining is abundant and strong in the myelin-rich structures of corpus callosum (cc) and hippocampus (hc). In contrast to this, there is significantly less PLP staining in the cc and hc of cathepsin D knockout (Ctsd–/–) mice. In the thalamus (thal) of Ctsd–/– mice, PLP staining is localized in clusters rather than in the fine fibrous structures seen in control mice. All stainings are representative examples of a series of experiments performed in Ctsd–/– ($n = 4$) and control mice ($n = 4$) at the age of 24 days. Scale bars, 150 μm. (b) Staining of the anterior commisura (ac) with antibodies against myelin proteins and Luxol fast blue (LFB). Both PLP and LFB stainings were reduced in the ac of Ctsd–/– mice compared with controls. Staining for myelin basic protein (MBP) revealed no major differences between the ac of control and Ctsd–/– mice. All stainings are representative examples of a series of experiments performed in Ctsd–/– ($n = 4$) and control mice ($n = 4$) at the age of 24 days. Scale bar, 200 μm.

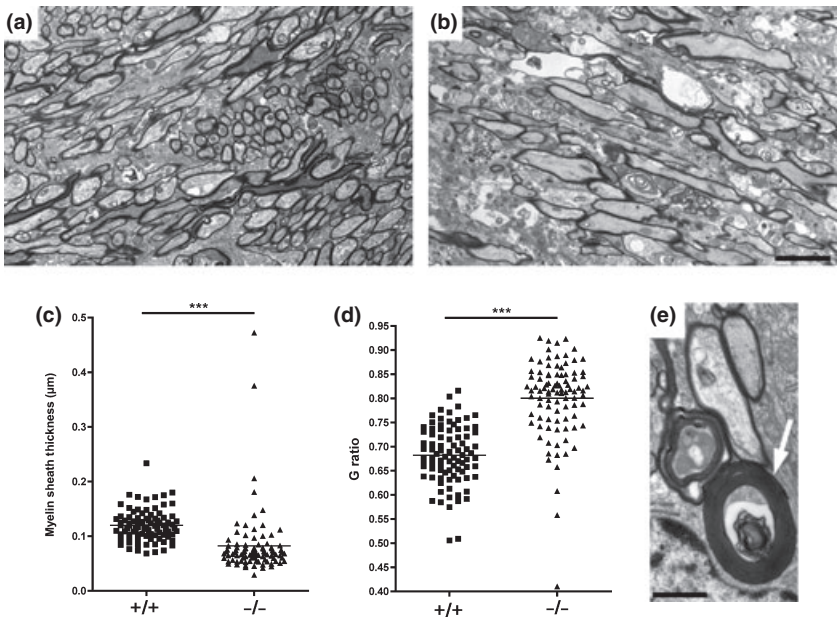

Fig. 2 Ultrastructural evidence for disrupted myelin in the corpus callosum of late-symptomatic (P23/24) *Ctsd*–/– mice. (a and b) Representative electron micrographs from the corpus callosum showing intact axons and myelin sheaths in littermate control mice (a) but reduced axon number, evidence for axon degeneration and disruption, as well as thinning of myelin sheaths in *Ctsd*–/– mice (b). Scale bar (a and b), 1 μm. (c) Scatter plot showing a significant decrease in the thickness of the myelin sheath in the corpus callosum of *Ctsd*–/– mice [***$p < 0.0001$, unpaired Mann–Whitney test; $n = 87$ axons from three control (+/+) and $n = 93$ axons from three *Ctsd*–/– (–/–) mice]. Note the outlier data points in the –/– showing evidence for hypermyelination of a small minority of axons. (d) Scatter plot showing a significant increase in the *g* ratio in the corpus callosum of *Ctsd*–/– mice [***$p < 0.0001$, unpaired Mann–Whitney test; $n = 87$ axons from three control (+/+) and $n = 93$ axons from 3 *Ctsd*–/– (–/–) mice]. (e) Electron micrograph showing a hypermyelinated axon (arrow) occasionally seen in the corpus callosum of *Ctsd*–/– mice. Scale bar, 500 nm.

many myelin sheaths appeared thinner than those in corresponding micrographs from control littermate mice. Quantitative measurements of myelin sheath thickness confirmed a significant reduction in *Ctsd*–/– mice (Fig. 2c; $p < 0.0001$, unpaired Mann–Whitney test). Interestingly, a small population of axon profiles in *Ctsd*–/– mice showed evidence of hypermyelination not present in control preparations (> 0.3 μm thick; Fig. 2e; also note data points at ~3.75 and ~4.75 μm in Fig. 2c). Myelin integrity in the corpus callosum was also assessed using *g* ratios. The *g* ratio (axon diameter : myelin sheath thickness × 2) is normally tightly regulated in healthy nerve fibers (Fraher and O'Sullivan 2000). The *g* ratios were significantly increased in *Ctsd*–/– mice compared with littermate controls (Fig. 2d; $p < 0.0001$, unpaired Mann–Whitney test), confirming that the observed reduction in myelin thickness was not simply occurring because of reduction in axonal diameter.

Proteomics

As the histochemical, immunohistochemical and morphological data suggested severe alterations in the myelin of *Ctsd*–/– mice, we next examined the myelin-related proteins by applying quantitative shotgun proteomics on synaptic fractions isolated from *Ctsd*–/– and control mice brains. About 500 proteins were identified in three parallel analyses of four different biological samples from both genotypes. A marked reduction of myelin-related proteins was evident from the proteomic analysis, whereas the quantity of proteins related to glucose metabolism were equally abundant in the *Ctsd*–/– and *Ctsd*+/+ mice, as summarized in Table 1. A highly significant reduction in the amount of three essential myelin proteins, PLP (0.59 × normal), MBP (0.51 × normal), and 2′,3′-cyclic nucleotide 3′-phosphodiesterase (CNP; 0.55 × normal) was observed in *Ctsd*–/– mice compared with controls at P24 (Table 1). The amount of peripheral myelin protein 22 also appeared reduced in the proteomic analyses but the result was not statistically significant. In addition, we noticed that the amount of ApoE, related to cholesterol transport, was increased ~2-fold in the affected brains (Table 1).

Lipid analyses

We next investigated if we would gain a further insight into the myelin-associated alterations by studying the lipid composition in *Ctsd*–/– mouse brains. Even in healthy vertebrate brain the myelination process markedly affects the brain lipid profile, and is highly dependent on the developmental stage. Therefore, the myelination process and also the

Table 1 Selected proteins related to myelin metabolism identified in the proteomic analysis of *Ctsd* knockout and wild-type mouse synaptosomes

Accession no	Name	Sequence coverage %	Ratio *Ctsd*−/−/*Ctsd*+/+	*p*
		Analysis I/II/III		
MYPR_MOUSE (P60202)	Myelin proteolipid protein	26/26/28	0.47/0.68/0.62	0.0000/0.0188/0.0000
MBP_MOUSE (P04370)	Myelin basic protein	32/44/40	0.57/0.52/0.44	0.0000*
CN37_MOUSE (P16330)	2′,3′-Cyclic nucleotide 3′-phosphodiesterase (EC 3.1.4.37)	42/47/45	0.58/0.59/0.47	0.0000*
APOE_MOUSE (P08226)	Apolipoprotein E precursor	38/40/N.D.	2.02/2.08/N.D.	0.0220/0.0001/N.D.
HXK1_MOUSE (P17710)	Hexokinase-1 (EC 2.7.1.1)	22/31/32	0.89/1.08/1.11	0.1082/0.2358/0.0020
KPYM_MOUSE (P52480)	Pyruvate kinase, isozyme M2 (EC 2.7.1.40)	31/68/38	1.03/1.11/0.93	0.8634/0.2456/0.2440
K6PP_MOUSE (Q9WUA3)	6-Phosphofructokinase type C (EC 2.7.1.11)	15/20/8	1.04/1.14/1.15	0.0037/0.1677/0.4780
NUAM_MOUSE (Q91VD9)	NADH-ubiquinone oxido-reductase 75 kDa subunit, mitochondrial precursor (EC 1.6.5.3.)	13/20/17	1.07/1.03/1.01	0.0003/0.6501/0.9190

Mass spectrometry based proteomic analysis was performed in three parallel experiments (I/II/III) in four different biological samples of each genotype as described in Materials and methods. Identification of the proteins is always based on multiple peptides. Table shows sequence coverage of each identified protein as percentages of the detected sequence of the total sequence in three parallel analysis. Quantitative comparison of each protein between the cathepsin D knockout and control mice is based on the results received from iTRAQ labeling (for more details see Materials and methods). Relative protein quantity differences are expressed as protein ratios (*Ctsd* ko/wt) in the three parallel analyses. Only if *p*-value of the quantitative analysis is less than 0.05, the protein ratio is statistically significant. *The same in all three analyses, N.D., not detected.

degradation of myelin can be monitored by studying the occurrence of these characteristics in the brain lipid profile.

We found several abnormalities in the lipid composition of *Ctsd*−/− mouse brains. The fatty acyl and alkenyl chain compositions in total lipids of *Ctsd*−/− mouse brains showed significantly reduced amounts of all individual plasmalogen-derived alkenyl chains and 20- and 24-carbon saturated and monounsaturated fatty acids typical for glycosphingolipids, as demonstrated by the PC analysis blot (Fig. 3a). The total mol% values for these indicators in *Ctsd*−/− mouse brain (rostral and caudal parts of cerebrum) were about two-thirds of those in the controls (Fig. 3b; statistically significant difference in each, Student's *t*-test). As myelin is known to be rich in plasmalogens and glycosphingolipids, the results suggest that the diseased brains have lost roughly one-third of their original myelin. The largest differences in the phospholipid molecular species profiles between *Ctsd*−/− and control mice were found in the ethanolamine plasmalogens (Fig. 3c; changes were more pronounced in the caudal part of cerebrum). In the *Ctsd*−/− brain, polyunsaturated plasmalogen species (alkenyl/acyl) 18:0/20:4, 18:1/20:4, 16:0/22:6, 18:0/22:5 and 18:0/22:6 were increased at the expense of all the species comprised of saturated and monounsaturated chains. These differences reflect changes in the relative amounts of different phosphatidylethanolamine (PE) plasmalogen pools of the brain (see Discussion). In addition, in phosphatidyl choline there were small 1-2 mol% increases in the 16:0/20:4 and 16:0/22:6 diacyl species, and the profiles of diacyl species of PE showed minor changes.

In our analyses, the total phospholipid and cholesterol content, calculated per total protein, appeared similar to controls in *Ctsd*−/− mouse brains (data not shown). However, a striking increase of cholesteryl esters and a reduction in triacylglycerols was found in the neutral lipid fraction of *Ctsd*−/− brains (Fig. 4). Cholesterol is an important structural component of myelin, and the turnover of cholesterol in the brain is slow. If present in excess, cholesterol may be stored intracellularly in the form of cholesteryl esters in lipid droplets.

To examine whether the observed alterations in cholesteryl esters were reflected in the protein machinery governing cholesterol homeostasis, we analyzed the protein amounts of ApoA–I, ApoE, and ABCA1 in P24 *Ctsd*−/− and control brains by semi-quantitative western blotting. The apoE protein amount was found to be increased 4-5 fold in *Ctsd*−/− tissue (Fig. 5a), in line with the elevated ApoE amounts observed by proteomics (Table 1). In contrast, a clear reduction in the protein amount of ABCA1 was found in *Ctsd*−/− brains (Fig. 5b). No change in the ApoA–I protein levels was observed (Fig. 5c).

Discussion

The myelin sheath is a layered membrane structure surrounding all myelinated axons in vertebrates. It is formed by oligodendrocytes, and it is essential for nerve conduction. In this work, we show multidisciplinary evidence for a marked disruption of myelin in the brains of *Ctsd*−/− mice.

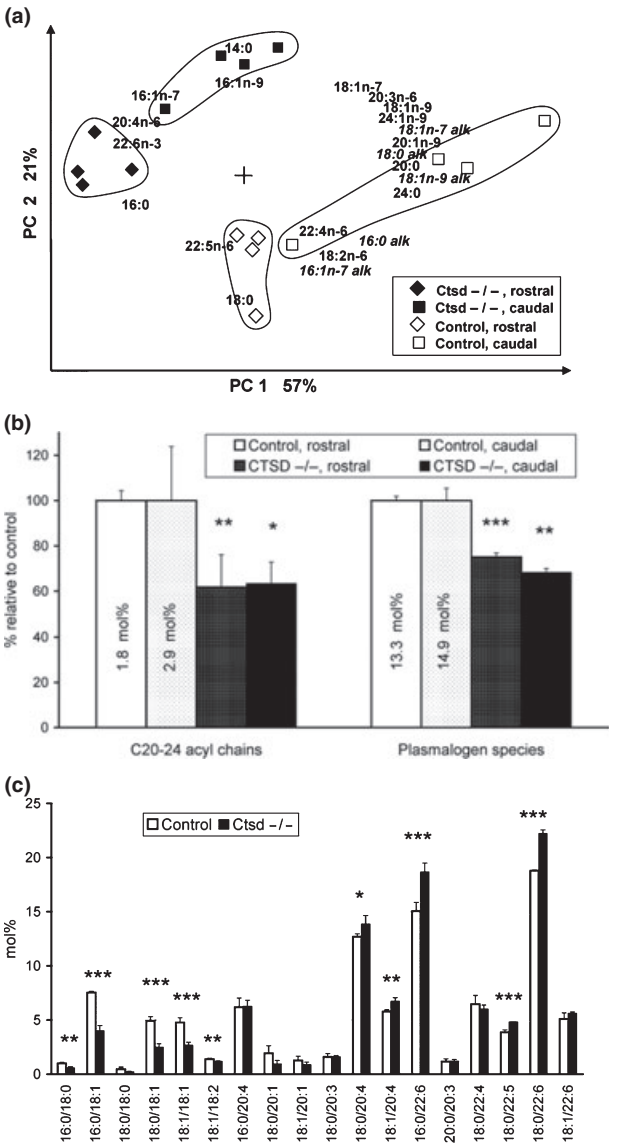

Fig. 3 Altered profiles of fatty acyl and alkenyl chains and PE plasmalogen species in the brains of *Ctsd*–/– mice. (a) The differences in the profile of acyl and alkenyl chains between the control and *Ctsd*–/– mouse brain samples are best demonstrated by using a multivariate approach, principal component analysis (PCA). PCA compressed the original high-dimensional data with minimal loss of information and presented the data points by using only two newly formed axes PC1 and PC2, which represented 57% and 21% of the total compositional variation among the samples, respectively (PC1 more important). The PCA biplot showed grouping of the samples of same origin and a clear-cut separation between the control and *Ctsd*–/– brain samples ($n = 4$ per genotype). Also, the rostral and caudal parts of the cerebrum were different. The larger the distance of any two samples (marked with symbols) on this biplot, the more they differ in terms of the whole profile of acyl and alkenyl chains. The abbreviated individual carbon chains situated far from the origin (marked with a cross in the middle of the plot) are responsible for the main part of the compositional difference and the ones closer to the origin have less separation power and importance. In addition, the brain samples farthest from the origin on one side were relatively rich in the acyl and alkenyl chains farthest on the same side (and relatively poor in the chains marked on the opposite side). The degree of coincidence of different acyl and alkenyl chains in all studied tissue samples can be read from the plot by drawing a connecting line between any two of those chains (variables) via the origin and then looking at the angle formed: e.g. 0°= total positive correlation, 90° = no correlation, 180° = total negative correlation (between the mol% of those two side chains in the studied brain samples). Based on these, the *Ctsd*–/– brains were relatively poor in all individual plasmalogen-derived alkenyl chains (in italics and denoted *alk*) and 20- and 24-carbon saturated and monounsaturated fatty acids characteristic for sphingolipids, but rich in polyunsaturated fatty acids 22:6*n*-3 and 20:4*n*-6. (b) The totals of the 20-24 carbon saturated and monounsaturated acyl chains and plasmalogen species (deduced from dimethylacetals formed from the plasmenyl chains) in the rostral and caudal parts of control and *Ctsd*–/– brain, expressed as percentages of the corresponding controls (*$p < 0.05$, **$p < 0.01$, and ***$p < 0.001$, Student's *t*-test). The mol% values of these indicators of all acyl chains or lipid molecular species of the control brain are indicated inside the control bars. (c) The main molecular species profiles of PE plasmalogens (the chains were marked in the order: alkenyl/acyl) in the control and *Ctsd*–/– brain, caudal part (statistics as in panel b); in the diseased brain, the polyunsaturated species were significantly increased at the expense of the monounsaturated ones.

Proteomic analyses indicated a significant loss of three major myelin proteins, PLP, MBP, and CNP. PLP is the most abundant structural component of myelin. PLP is responsible for the maintenance of myelin stability and axonal integrity (Boison and Stoffel 1994; Hobson *et al.* 2002), and it has also been shown to interact with cholesterol (Krämer-Albers *et al.* 2000). MBP is the second most abundant protein of the CNS myelin, comprising as much as 30% of its total protein (Boggs 2006). It is essential in the assembly of myelin, indicated by the lack of compact myelin in mice and rats with mutations in MBP gene (Boggs 2006). CNP is a myelin-associated enzyme that makes up ~4% of total CNS myelin protein, and it catalyzes the phosphodiester hydrolysis of 2′,3′-cyclic nucleotides. CNP is an early marker of oligodendrocyte differentiation, while MBP is important for oligodendrocyte morphogenesis at later stages of differentiation (Galiano *et al.* 2006). In good accordance with the proteomic analysis, PLP staining was markedly reduced in *Ctsd*–/– brains compared with controls. Staining for MBP, however, was unable to show major alterations between the control and affected mouse brain, although quantitative analysis revealed a significant reduction of the MBP protein in the *Ctsd*–/– brain.

The reduced amounts of the essential myelin proteins are well in line with our EM findings showing significant thinning of axonal myelin sheets and axonal degeneration in *Ctsd*–/– mice, suggesting that demyelination occurs in the corpus callosum of *Ctsd*–/– mice. We also found evidence

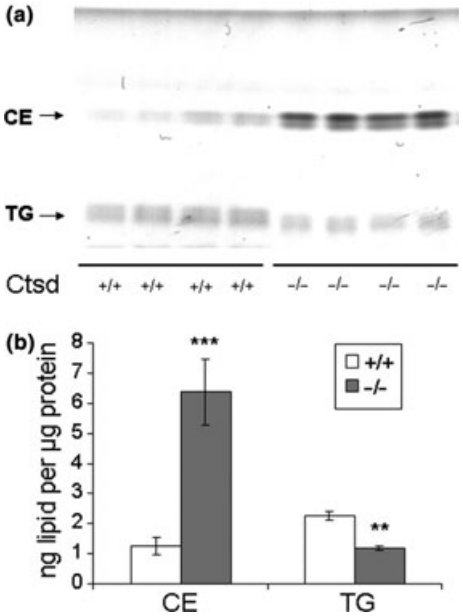

Fig. 4 Cholesteryl esters accumulate and triacylglycerols decrease in the brains of *Ctsd* deficient mice. (a) Lipids were extracted from P24 *Ctsd* wild-type (+/+) and knockout (−/−) mice frontal lobes and analyzed with HPTLC as detailed in Materials and methods. Lipids were identified by comparing their migration to known standards. CE, cholesteryl esters; TG, triacylglycerols. (b) The HPTLC plates were scanned and quantified in comparison to known amounts of standard lipids; $n = 4$ samples from two individuals per genotype; wild-type (+/+), knockout (−/−), $^{***}p < 0.001$, $^{**}p < 0.005$; error bars, SEM.

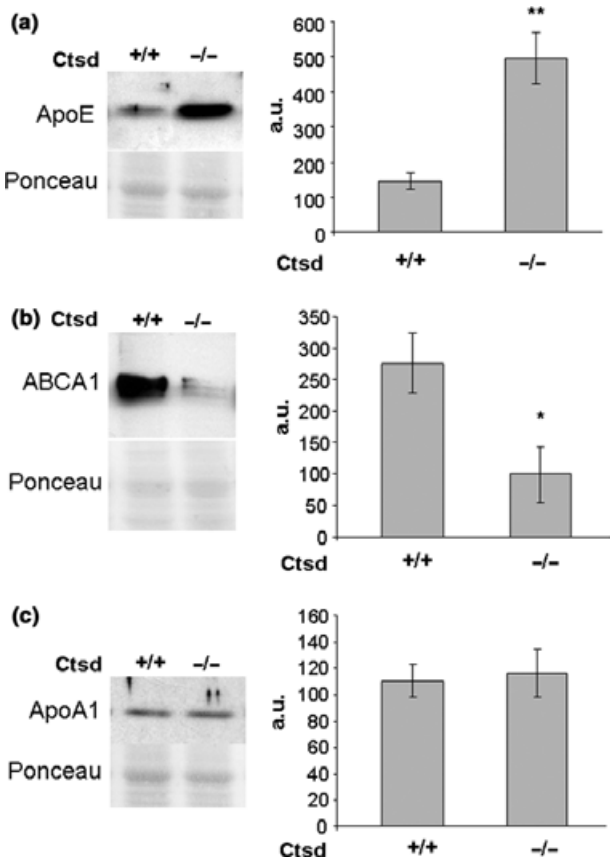

Fig. 5 The amount of ApoE protein is increased and that of ABCA1 decreased in the brains of *Ctsd* deficient mice. Aliquots of brain lysates from wild-type (+/+) and *Ctsd* knockout (−/−) mice (20 µg of protein lysate from each) were analyzed by western blotting using antibodies against ApoE, ABCA1, or ApoA1. ABCA1 samples were separated by 6% sodium dodecyl sulfate–polyacrylamide gel electrophoresis, ApoA1 and ApoE samples by 10-12% sodium dodecyl sulfate–polyacrylamide gel electrophoresis. The band intensities were quantified; $^{*}p < 0.05$ and $^{**}p < 0.005$, $n = 4$ samples from two individuals per genotype, except for ApoA1 $n = 5$ individuals per genotype. a.u., arbitrary units; error bars, SEM.

for a small population of hypermyelinated axons, strengthening the idea that the normally tightly regulated myelination process is disrupted in *Ctsd*−/− mice. Importantly, the increased *g* ratios observed indicate that the reduction in myelin thickness was not simply occurring because of a corresponding reduction in axonal diameter in *Ctsd*−/− mice.

Myelin assembly is a multi-step process: It starts already during the transport of myelin proteins and lipids through the biosynthetic pathway and continues at the plasma membrane aided by MBP (Simons and Trotter 2007). At P24, PLP staining was reduced in *Ctsd*−/− brains, but appeared relatively normal at P16 and P19 (data not shown). Apparently, the difference in PLP staining arises between P19 and P24, simultaneously with other pathological changes such as gliosis, magnetic resonance imaging changes and loss of synapses in distinct brain areas (Haapanen *et al.* 2007; Partanen *et al.* 2008). This is also a period of active myelination. Therefore, it is possible that the decrease in myelin content in *Ctsd*−/− mice may not only result from myelin degradation, but also from a delay or failure in myelin assembly. These two processes, degradation of myelin and abnormal myelin assembly, may occur simultaneously in *Ctsd*−/− mice. In fact, the existence of hypermyelinated and degenerating axons in the corpus callosum of *Ctsd*−/− mice favor this idea. Moreover, characteristics of developmental delay exist in the newborns and lambs with CTSD deficiency (Fritchie *et al.* 2008; Tyynelä *et al.*, unpublished data).

The myelination process has major effects on lipid profiles of the vertebrate brain, with increases e.g. in alkenyl-acyl species of phosphatidylethanolamines and in glycosphingolipids with 20- and 24-carbon acyl chains (Rao 1977; Martinez 1982). Moreover, altered concentrations of plasmalogens and glycosphingolipids have been reported in several neurological diseases, such as Alzheimer's disease, adrenoleukodystrophy, and sphingolipidoses (Ozkara 2004; Hartmann *et al.* 2007; Khan *et al.* 2008). We found indications of significant net reduction in the total plasmalogen and glycosphingolipid content, as well as altered molecular species profiles of ethanolamine plasmalogens in *Ctsd*−/−

brain. These findings suggest a marked decrease, either because of increased degradation or decreased synthesis, in the myelin content of *Ctsd*−/− mouse brains. In the human white matter, 50% or more of the ethanolamine plasmalogens were reported to consist of molecular species with monounsaturated acyl chains, whereas in gray matter, only 20-30% of these lipids were comprised of monounsaturated species, and polyunsaturated species dominated instead (Han *et al.* 2001). Thus, the observed reduction in the monounsaturated species and the concomitant increase in the polyunsaturated species in *Ctsd*−/− mice can be explained by a decrease in the brain content of white matter, i.e. myelin. The decreased tissue levels of plasmalogens and glycolipids (largely galactolipids) may simply mirror a reduction in the brain myelin content. Importantly, defects in the metabolism of myelin lipids may also be a factor accelerating myelin degradation, because mice that are not able to synthesize galactolipids or are plasmalogen-deficient develop drastic hypomyelination (Hirahara *et al.* 2004; Gorgas *et al.* 2006).

Previous evidence for altered glycosphingolipid metabolism in CTSD deficiencies comes from two directions: First, the amount of sphingolipid activator protein (SAP) precursor was found to be reduced in the brains of *Ctsd*−/− mice (Jabs *et al.* 2008). This protein precursor gives rise to SAP A–D, which facilitate the lysosomal turnover of most glycosphingolipids. Second, accumulation of SAP D-positive inclusions in the CNS is a pathological hallmark of human and ovine CTSD deficiencies (Tyynela *et al.* 2000; Siintola *et al.* 2006; Fritchie *et al.* 2008). It has been suggested that CTSD may be involved in the processing of SAP precursor and hence cause these abnormalities (Jabs *et al.* 2008). Alternatively, in the light of our present results, the reduced amount of SAP precursor and the pathological accumulation of SAP D may be a consequence of severely decreased tissue levels of glycolipids.

The structural alterations and reduction of myelin were associated with a marked increase of cholesteryl esters within the brains of *Ctsd*−/− mice. Increase in cholesteryl esters serves as a detoxification mechanism for excess free cholesterol (Yao and Tabas 2001). The enzyme responsible for cholesterol esterification, acyl coenzyme A:cholesterol acyltransferase, is expressed only at low levels in the CNS (Uelmen *et al.* 1995) and in line with this, essentially all cholesterol in the CNS is in the unesterified form under normal conditions (Bjorkhem and Meaney 2004). However, degradation of myelin might release an excess of free cholesterol, which then might become converted to cholesteryl esters. In addition to increased cholesteryl esters, triacylglycerols were found to be markedly decreased in terminal *Ctsd*−/− brains. Triacylglycerols constitute a major source of energy in many tissues but in the CNS, which relies on glucose and ketone bodies for energy, their content is low (Macala *et al.* 1983). The decrease of triacylglycerols observed in *Ctsd*−/− brains may, however, be linked to the cholesterol imbalance: The fatty acyls are needed to store cholesterol as cholesteryl ester may have been derived from degraded triacylglycerols.

In addition, alterations were found in the content of ApoE and ABCA1, key proteins related to cholesterol transport in the CNS (Pitas *et al.* 1987; Karasinska *et al.* 2009). Recently, reduced CTSD activity was shown to be associated with reduced expression of ABCA1, and CTSD was shown to regulate ABCA1 mediated lipid efflux and high-density lipoprotein cholesterol levels (Haidar *et al.* 2006). These observations are in line with our findings, showing a dramatic reduction of ABCA1 in P24 *Ctsd*−/− mouse brains. Increase in the amount of ApoE in *Ctsd*−/− mouse brains may reflect the increased activity of CNS lipoprotein synthesizing cells in an attempt to clear the excess free cholesterol resulting from the breakdown of myelin. Alternatively, the increased expression of ApoE may reflect the fact that after injury, ApoE expression is elevated and also found in cell populations that normally do not express it (Xu *et al.* 2006). Additionally, CTSD has been implicated in the proteolysis of ApoE (Zhou *et al.* 2006), and hence, perturbed degradation is yet another possible explanation for the increase of ApoE. ApoE-containing nascent lipoprotein particles secreted by astrocytes are in part lipidated by ABCA1 (Hirsch-Reinshagen *et al.* 2004; Wahrle *et al.* 2004). As CTSD deficiency leads to a marked down-regulation of ABCA1, astrocytes are likely to be unable to produce sufficiently lipidated lipoprotein particles. As a consequence, the intracellular storage of cholesterol as cholesteryl ester would be increased.

In conclusion, we show the first evidence for a marked disruption of myelin in the brains of *Ctsd*−/− mice. This is in agreement with findings in other species with CTSD deficiency. In parallel, hypermyelination and altered myelin integrity was observed in *Ctsd*−/− mice. Structural alterations of myelin were associated with an unforeseen accumulation of cholesteryl esters and abnormal fatty acyl and alkenyl chain profiles within the brains of *Ctsd*−/− mice, suggesting that pronounced degradation of myelin is occurring in the brains of these mice at P24, possibly simultaneously with aberrant myelin assembly. In addition, the abnormal levels of proteins related to cholesterol transport suggest that the overall trafficking of cholesterol is distorted in the brains of *Ctsd*−/− mice and emphasize the role of CTSD in the regulation of lipid homeostasis. These data suggest that alterations in lipid metabolism may play an important role in the process leading to neurodegeneration in CTSD deficiencies.

Acknowledgements

We wish to thank Professor Paul Saftig (University of Kiel, Germany) for Cathepsin D knockout mice and fruitful discussions.

This study was financially supported by The Academy of Finland (Grants 111261 and 129148 to RK, 214343 to JT, and 123743 to EI) and the European Union (EU-Lshm-CT2003-503051 to JT).

References

Bartlett E. M. and Lewis D. H. (1970) Spectrophotometric determination of phosphate esters in the presence and absence of orthophosphate. *Anal. Biochem.* **36**, 159–167.

Bjorkhem I. and Meaney S. (2004) Brain cholesterol: long secret life behind a barrier. *Arterioscler. Thromb. Vasc. Biol.* **24**, 806–815.

Bligh E. G. and Dyer W. J. (1959) A rapid method of total lipid extraction and purification. *Can. J. Biochem. Physiol.* **37**, 911–917.

Boggs J. M. (2006) Myelin basic protein: a multifunctional protein. *Cell. Mol. Life Sci.* **63**, 1945–1961.

Boison D. and Stoffel W. (1994) Disruption of the compacted myelin sheath of axons of the central nervous system in proteolipid protein-deficient mice. *Proc. Natl Acad. Sci. USA* **91**, 11709–11713.

Cargile B. J., Talley D. L. and Stephenson J. L. Jr (2004) Immobilized pH gradients as a first dimension in shotgun proteomics and analysis of the accuracy of pI predictability of peptides. *Electrophoresis* **25**, 936–945.

Folch J., Lees M. and Sloane Stanley G. H. (1957) A simple method for the isolation and purification of total lipides from animal tissues. *J. Biol. Chem.* **226**, 497–509.

Fraher J. P. and O'Sullivan A. W. (2000) Interspecies variation in axon-myelin relationships. *Cells Tissues Organs* **167**, 206–213.

Fritchie K., Siintola E., Armao D. *et al.* (2008) Novel mutation and the first prenatal screening of cathepsin D deficiency (CLN10). *Acta Neuropathol.* **117**, 201–208.

Gamble W., Vaughan M., Kruth H. S. and Avigan J. (1978) Procedure for determination of free and total cholesterol in micro- or nanogram amounts suitable for studies with cultured cells. *J. Lipid Res.* **19**, 1068–1070.

Galiano M. R., Andrieux A., Deloulme J. C., Bosc C., Schweitzer A., Job D. and Hallak M. E. (2006) Myelin basic protein functions as a microtubule stabilizing protein in differentiated oligodendrocytes. *J. Neurosci. Res.* **84**, 534–541.

Garborg I., Torvik A., Hals J., Tangsrud S. E. and Lindemann R. (1987) Congenital neuronal ceroid lipofuscinosis. A case report. *Acta Pathol. Microbiol. Immunol. Scand. A* **95**, 119–125.

Gillingwater T. H., Ingham C. A., Parry K. E., Wright A. K., Haley J. E., Wishart T. M., Arbuthnott G. W. and Ribchester R. R. (2006) Delayed synaptic degeneration in the CNS of Wlds mice after cortical lesion. *Brain* **129**, 1546–1556.

Gorgas K., Teigler A., Komljenovic D. and Just W. W. (2006) The ether lipid-deficient mouse: tracking down plasmalogen functions. *Biochim. Biophys. Acta* **1763**, 1511–1526.

Haapanen A., Ramadan U. A., Autti T., Joensuu R. and Tyynela J. (2007) *In vivo* MRI reveals the dynamics of pathological changes in the brains of cathepsin D-deficient mice and correlates changes in manganese-enhanced MRI with microglial activation. *Magn. Reson. Imaging* **25**, 1024–1031.

Haidar B., Kiss R. S., Sarov-Blat L., Brunet R., Harder C., McPherson R. and Marcel Y. L. (2006) Cathepsin D, a lysosomal protease, regulates ABCA1-mediated lipid efflux. *J. Biol. Chem.* **281**, 39971–39981.

Haimi P., Uphoff A., Hermansson M. and Somerharju P. (2006) Software tools for analysis of mass spectrometric lipidome data. *Anal. Chem.* **78**, 8324–8331.

Han X., Holtzman D. M. and McKeel D. W. Jr (2001) Plasmalogen deficiency in early Alzheimer's disease subjects and in animal models: molecular characterization using electrospray ionization mass spectrometry. *J. Neurochem.* **77**, 1168–1180.

van Haperen R., van Tol A., Vermeulen P., Jauhiainen M., van Gent T., van den Berg P., Ehnholm S., Grosveld F., van der Kamp A. and de Crom R. (2000) Human plasma phospholipid transfer protein increases the antiatherogenic potential of high density lipoproteins in transgenic mice. *Arterioscler. Thromb. Vasc. Biol.* **20**, 1082–1088.

Hartmann T., Kuchenbecker J. and Grimm M. O. (2007) Alzheimer's disease: the lipid connection. *J. Neurochem.* **103**(Suppl. 1), 159–170.

Hermansson M., Uphoff A., Kakela R. and Somerharju P. (2005) Automated quantitative analysis of complex lipidomes by liquid chromatography/mass spectrometry. *Anal. Chem.* **77**, 2166–2175.

Hirahara Y., Bansal R., Honke K., Ikenaka K. and Wada Y. (2004) Sulfatide is a negative regulator of oligodendrocyte differentiation: development in sulfatide-null mice. *Glia* **45**, 269–277.

Hirsch-Reinshagen V., Zhou S., Burgess B. L., Bernier L., McIsaac S. A., Chan J. Y., Tansley G. H., Cohn J. S., Hayden M. R. and Wellington C. L. (2004) Deficiency of ABCA1 impairs apolipoprotein E metabolism in brain. *J. Biol. Chem.* **279**, 41197–41207.

Hobson Z., Huang K., Sperle D. L., Stabley H. G., Marks F. and Cambi A. (2002) PLP splicing abnormality is associated with an unusual presentation of PMD. *Ann. Neurol.* **52**, 477–488.

Jabs S., Quitsch A., Kakela R. *et al.* (2008) Accumulation of bis(monoacylglycero)phosphate and gangliosides in mouse models of neuronal ceroid lipofuscinosis. *J. Neurochem.* **106**, 1415–1425.

Jurevics H. and Morell P. (1995) Cholesterol for synthesis of myelin is made locally, not imported into brain. *J. Neurochem.* **64**, 895–901.

Kainu V., Hermansson M. and Somerharju P. (2008) Electrospray ionization mass spectrometry and exogenous heavy isotope-labeled lipid species provide detailed information on aminophospholipid acyl chain remodeling. *J. Biol. Chem.* **283**, 3676–3687.

Kakela R., Somerharju P. and Tyynela J. (2003) Analysis of phospholipid molecular species in brains from patients with infantile and juvenile neuronal-ceroid lipofuscinosis using liquid chromatography-electrospray ionization mass spectrometry. *J. Neurochem.* **84**, 1051–1065.

Kakela R., Kakela A., Kahle S., Becker P. H., Kelly A. and Furness R. W. (2005) Fatty acid signatures in plasma of captive herring gulls as indicators of demersal or pelagic fish diet. *Mar. Ecol. Prog. Ser.* **293**, 191–200.

Karasinska J. M., Rinninger F., Lutjohann D. *et al.* (2009) Specific loss of brain ABCA1 increases brain cholesterol uptake and influences neuronal structure and function. *J. Neurosci.* **29**, 3579–3589.

Khan M., Singh J. and Singh I. (2008) Plasmalogen deficiency in cerebral adrenoleukodystrophy and its modulation by lovastatin. *J. Neurochem.* **106**, 1766–1779.

Koike M., Nakanishi H., Saftig P. *et al.* (2000) Cathepsin D deficiency induces lysosomal storage with ceroid lipofuscin in mouse CNS neurons. *J. Neurosci.* **20**, 6898–6906.

Krämer-Albers E. M., Gehrig-Burger K., Thiele C., Trotter J. and Nave K. A. (2006) Perturbed interactions of mutant proteolipid protein/DM20 with cholesterol and lipid rafts in oligodendroglia: implications for dysmyelination in spastic paraplegia. *J. Neurosci.* **26**, 11743–11752.

Kvalheim O. M. and Karstang T. V. (1987) A general-purpose program for multivariate data analysis. *Chemom. Intell. Lab. Syst.* **2**, 235–237.

Lowry O. H., Rosebrough N. J., Farr A. L. and Randall R. J. (1951) Protein measurement with the Folin phenol reagent. *J. Biol. Chem.* **193**, 265–275.

Macala L. J., Yu R. K. and Ando S. (1983) Analysis of brain lipids by high performance thin-layer chromatography and densitometry. *J. Lipid Res.* **24**, 1243–1250.

Martinez M. (1982) Myelin lipids in the developing cerebrum, cerebellum, and brain stem of normal and undernourished children. *J. Neurochem.* **39**, 1684–1692.

Norman R. and Wood N. (1941) Congenital form of amaurotic family idiocy. *J. Neur. Psychiat.* **4**, 175–190.

Ozkara H. A. (2004) Recent advances in the biochemistry and genetics of sphingolipidoses. *Brain Dev.* **26**, 497–505.

Partanen S., Haapanen A., Kielar C., Pontikis C., Alexander N., Inkinen T., Saftig P., Gillingwater T. H., Cooper J. D. and Tyynela J. (2008) Synaptic changes in the thalamocortical system of cathepsin D-deficient mice: a model of human congenital neuronal ceroid-lipofuscinosis. *J. Neuropathol. Exp. Neurol.* **67**, 16–29.

Pitas R. E., Boyles J. K., Lee S. H., Foss D. and Mahley R. W. (1987) Astrocytes synthesize apolipoprotein E and metabolize apolipoprotein E-containing lipoproteins. *Biochim. Biophys. Acta* **917**, 148–161.

Rao P. S. (1977) Fatty acids of cerebrosides in different regions of the developing foetal brain. *Lipids* **12**, 335–339.

Ross P. L., Huang Y. N., Marchese J. N. *et al.* (2004) Multiplexed protein quantitation in Saccharomyces cerevisiae using amine-reactive isobaric tagging reagents. *Mol. Cell Proteomics* **3**, 1154–1169.

Saftig P., Hetman M., Schmahl W. *et al.* (1995) Mice deficient for the lysosomal proteinase cathepsin D exhibit progressive atrophy of the intestinal mucosa and profound destruction of lymphoid cells. *EMBO J.* **14**, 3599–3608.

Saher G., Brugger B., Lappe-Siefke C., Mobius W., Tozawa R., Wehr M. C., Wieland F., Ishibashi S. and Nave K. A. (2005) High cholesterol level is essential for myelin membrane growth. *Nat. Neurosci.* **8**, 468–475.

Siintola E., Partanen S., Stromme P., Haapanen A., Haltia M., Maehlen J., Lehesjoki A. E. and Tyynela J. (2006) Cathepsin D deficiency underlies congenital human neuronal ceroid-lipofuscinosis. *Brain* **129**, 1438–1445.

Simons M. and Trotter J. (2007) Wrapping it up: the cell biology of myelination. *Curr. Opin. Neurobiol.* **17**, 533–540.

Suopanki J., Lintunen M., Lahtinen H., Haltia M., Panula P., Baumann M. and Tyynela J. (2002) Status epilepticus induces changes in the expression and localization of endogenous palmitoyl-protein thioesterase 1. *Neurobiol. Dis.* **10**, 247–257.

Tyynela J., Sohar I., Sleat D. E., Gin R. M., Donnelly R. J., Baumann M., Haltia M. and Lobel P. (2000) A mutation in the ovine cathepsin D gene causes a congenital lysosomal storage disease with profound neurodegeneration. *EMBO J.* **19**, 2786–2792.

Uelmen P. J., Oka K., Sullivan M., Chang C. C., Chang T. Y. and Chan L. (1995) Tissue-specific expression and cholesterol regulation of acylcoenzyme A:cholesterol acyltransferase (ACAT) in mice. Molecular cloning of mouse ACAT cDNA, chromosomal localization, and regulation of ACAT *in vivo* and *in vitro*. *J. Biol. Chem.* **270**, 26192–26201.

Wahrle S. E., Jiang H., Parsadanian M., Legleiter J., Han X., Fryer J. D., Kowalewski T. and Holtzman D. M. (2004) ABCA1 is required for normal central nervous system ApoE levels and for lipidation of astrocyte-secreted apoE. *J. Biol. Chem.* **279**, 40987–40993.

Xu Q., Bernardo A., Walker D., Kanegawa T., Mahley R. W. and Huang Y. (2006) Profile and regulation of apolipoprotein E (ApoE) expression in the CNS in mice with targeting of green fluorescent protein gene to the ApoE locus. *J. Neurosci.* **26**, 4985–4994.

Yao P. M. and Tabas I. (2001) Free cholesterol loading of macrophages is associated with widespread mitochondrial dysfunction and activation of the mitochondrial apoptosis pathway. *J. Biol. Chem.* **276**, 42468–42476.

Zhou W., Scott S. A., Shelton S. B. and Crutcher K. A. (2006) Cathepsin D-mediated proteolysis of apolipoprotein E: possible role in Alzheimer's disease. *Neuroscience* **143**, 689–701.

